EXPERIMENTAL CELL RESEARCH 318 (2012) 653–661

Available online at www.sciencedirect.com

SciVerse ScienceDirect

www.elsevier.com/locate/yexcr

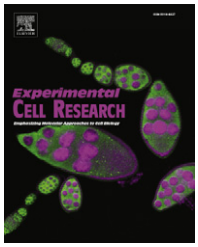

Research Article

Fused in sarcoma (FUS) interacts with the cytolinker protein plectin: Implications for FUS subcellular localization and function

Christer Thomsen[a], *Sameer Udhane*[a], *Rikard Runnberg*[a], *Gerhard Wiche*[b], *Anders Ståhlberg*[a], *Pierre Åman*[a,*]

[a]*Sahlgrenska Cancer Center, Department of Pathology, Sahlgrenska Academy at the University of Gothenburg, Box 425, 40530, Gothenburg, Sweden*
[b]*Department of Biochemistry and Cell Biology, Max F. Perutz Laboratories, University of Vienna, Dr. Bohr-Gasse 9/5, A-1030, Vienna, Austria*

ARTICLE INFORMATION

Article Chronology:
Received 23 September 2011
Revised version received 21 December 2011
Accepted 24 December 2011
Available online 4 January 2012

Keywords:
FUS
TLS
Plectin
RNA transport
Amyotrophic lateral sclerosis
Epidermolysis bullosa

ABSTRACT

Fused in sarcoma (FUS) is a multifunctional protein involved in transcriptional control, pre-mRNA processing, RNA transport and translation. The domain structure of FUS reflects its functions in gene regulation and its ability to interact with other proteins, RNA and DNA. By use of a recombinant fragment of FUS in pull-down experiments followed by mass spectrometry analysis we have identified a novel interaction between the FUS N-terminal and the cytolinker plectin. An *in situ* proximity ligation assay confirmed that FUS-plectin interactions take place in the cytoplasm of cells. Furthermore, plectin deficient cells showed an altered subcellular localization of FUS and a deregulated expression of mRNAs bound to FUS. Our results show that plectin is important for normal FUS localization and function. Mutations involving FUS are causative factors in sarcomas and leukemias and also hereditary forms of amyotrophic lateral sclerosis and frontotemporal lobar degeneration. Plectin deficiency causes epidermolysis bullosa, a disease involving the skin and neuromuscular system. The novel FUS-plectin interaction offers new perspectives for understanding the role of FUS and plectin mutations in the pathogenesis of these diseases.

Introduction

FUS (fused in sarcoma), also known as *TLS* (translocated in liposarcoma), was initially discovered as part of the fusion oncogene *FUS-DDIT3* in myxoid liposarcoma [1–3]. Genetic rearrangement fusing the 5′ part of *FUS* with genes encoding various transcription factors is a recurrent event in sarcomas and leukemias [4]. Recently, *FUS* mutations have also been implicated in familial forms of the neurodegenerative disorders amyotrophic lateral sclerosis (ALS) and frontotemporal lobar degeneration (FTLD) [5–7]. The *FUS* gene encodes a ubiquitously expressed 526 amino acid protein with a central RNA recognition motif and a C-terminal zinc finger with potential protein and DNA binding capacity [8–10]. Sequence homology includes FUS in the FET family, whose members (FUS,

* *Corresponding author.* Fax: +46 31828733.
E-mail addresses: christer.thomsen@llcr.med.gu.se (C. Thomsen), sameer.udhane@dkf.unibe.ch (S. Udhane), rikard.runnberg@gu.se (R. Runnberg), gerhard.wiche@univie.ac.at (G. Wiche), anders.stahlberg@neuro.gu.se (A. Ståhlberg), pierre.aman@llcr.med.gu.se (P. Åman).

Abbreviations: ABD, actin binding domain; ALS, amyotrophic lateral sclerosis; EB, epidermolysis bullosa; eGFP, enhanced green fluorescent protein; FTLD, frontotemporal lobar degeneration; IFBD, intermediate filament binding domain; ko, knockout; MS, mass spectrometry; NTD, N-terminal domain; RD, repeat domain; RGG, RGG repeat domain; RRM, RNA recognition motif; PLA, proximity ligation assay; SEM, standard error of mean; wt, wildtype; ZF, zinc finger domain.

0014-4827/$ – see front matter © 2012 Elsevier Inc. All rights reserved.
doi:10.1016/j.yexcr.2011.12.019

EWSR1 and TAF15) are RNA-binding proteins involved in several levels of gene regulation [4,11,12]. FUS is implicated in regulation of gene promoter activity [13,14], pre-mRNA splicing [15] and shuttles between the nucleus and cytoplasm bound to RNA [16]. The FET proteins bind thousands of distinct mRNAs with a large overlap between the three proteins [17]. The cellular distribution of FUS is predominantly nuclear, but this varies between specific tissues and cell types [16,18]. The variability in subcellular localization probably reflect cell type specific requirements, for instance FUS has been shown to transport specific mRNAs to neuronal dendritic spines [19,20]. The subcellular localization is dynamically regulated as stress conditions trigger accumulation of FUS in cytoplasmic stress granules involved in translational control [18,21]. *FUS* mutations in ALS and FTLD cause the formation of cytoplasmic and nuclear FUS immunoreactive inclusion bodies in diseased tissue and cultured cells [22,23]. Mutations in the proximal C-terminus of FUS have further been reported to impair FUS transport over the nuclear membrane and promote cytoplasmic accumulation [22,23]. Although, ALS and FTLD linked mutations in the central and N-terminal part of FUS remain uncharacterized, proper localization and function of FUS are presumed to be required for normal function of neurons [5–7]. The FUS N-terminal domain (NTD), also expressed in chimeric fusion oncoproteins, is mainly composed of SYGQ enriched degenerate repeats [4] and predicted to have a disordered structure [24]. In the context of fusion oncoproteins, the FUS NTD has been described as a transcriptional activation domain. However, the role of the FUS NTD and its contribution to function of wildtype FUS is not well understood. As intrinsically disordered protein domains are important mediators of protein–protein interactions [25] we utilized a recombinant fragment of the FUS NTD in a pull-down screening approach. We have identified the cytolinker plectin as a novel interaction partner of FUS, and characterized the subcellular localization where FUS–plectin association occurs. Furthermore, we demonstrate that plectin is required for the correct nucleocytoplasmic distribution of FUS and that FUS interacting mRNAs are deregulated in plectin deficient cells.

Material and methods

Cell cultures

The Raji lymphoma and HT1080 fibrosarcoma cell lines were cultured in RPMI1640 with 2 mM L-Glutamine, primary mouse fibroblasts were grown in DMEM Glutamax. All culture media was supplemented with 10% FBS, 50 U/mL penicillin and 50 μg/mL streptomycin. Stable expression of FUS-eGFP in modified HT1080 cells [18] was maintained by addition of 500 μg/mL Geniticin. All reagents for cell culture were obtained from Invitrogen. For immunofluorescence and proximity ligation assay analysis cells were cultured in 4 or 8 well chamber slides respectively (Nunc). Stress granule formation was induced by treatment with 0.5 mM sodium arsenite (Sigma-Aldrich) for 15–60 min.

Expression and preparation of GST-6xHis fusion proteins

The cDNA sequences encoding FUS amino acids 1–175 (FUS NTD), EWSR1 amino acids 1–264 (EWSR1 NTD) and TAF15 amino acids 1–201 (TAF15 NTD) were amplified by PCR, and subcloned to a pQE60 expression vector (Qiagen) modified to express a GST-6xHis tandem tag downstream of the cloning site. The coding regions of vectors were verified by DNA sequencing using BigDye Terminator v1.1 (Applied Biosystems). GST-tagged protein domains were expressed in the Rosetta DE3 pLysS bacterial strain (Novagen) at 37 °C for 4 h after induction with 1 mM IPTG at 0.6 OD_{600}. Cultures were harvested by centrifugation, frozen in liquid nitrogen and stored at −80 °C. Bacteria were resuspended in ice-cold lysis buffer (50 mM NaH_2PO_4 pH7.5, 0.5% NP-40, 300 mM NaCl and 5 mM dithiothreitol) with protease inhibitors (Complete Mini, Roche Diagnostics) and sonicated. Crude lysates were cleared by centrifugation at 12,000 rcf for 20 min at 4 °C and incubated with pre-equilibrated Glutathione Sepharose 4B (GE Healthcare) in batch mode for 15 min at 4 °C. The sepharose was washed 4 times with wash buffer (50 mM NaH_2PO_4 pH7.5, 1% NP-40, 500 mM, 10% glycerol and 1 mM dithiothreitol), 2 times with lysis buffer without dithiothreitol and stored overnight at 4 °C.

Pull-down assays

Raji cells were collected by centrifugation, washed in PBS, and lysed in ice-cold protein binding buffer (20 mM Tris pH7.5, 0.5% NP-40, 100 mM NaCl and 2 mM $MgCl_2$) with protease inhibitors (Complete Mini, Roche Diagnostics) at a concentration of 5-10×10^6 cells per mL. Cell lysis was facilitated by end-over-end mixing for 15 min at 4 °C and protein extracts were subsequently cleared by centrifugation at 12,000 rcf for 20 min at 4 °C. Sepharose with bound GST-tagged protein was equilibrated in protein binding buffer and incubated with Raji protein extract, corresponding to 25-50×10^6 cells per sample, with end-over-end mixing for 3 h at 4 °C. The sepharose was washed 4 times with protein binding buffer, and immobilized protein complexes were eluted by denaturation in 2× LDS Sample Buffer (Invitrogen) at 95 °C for 10 min.

Subcellular fractionation

Mouse fibroblasts were kept in culture for 48 h and subsequently harvested and processed with the PARIS kit (Ambion) according to the manufacturers' instructions. For each sample, 5×10^5 cells were used to generate protein and RNA samples from whole cells or cytoplasmic and nuclear fractions.

SDS-PAGE and Western blotting

Protein samples were mixed with LDS Sample Buffer and Sample Reducing Agent according to the manufacturers' instructions. Samples were denatured at 70 °C for 10 min, separated on NuPAGE 4–12% Bis-Tris or 3–8% Tris-Acetate gels, and either stained with SimplyBlue SafeStain or transferred to PVDF membranes by wet blot. All reagents for SDS-PAGE and blotting were obtained from Invitrogen. PVDF membranes were blocked with 5% w/v skim milk in TBS-T (50 mM Tris–HCl pH 6.8, 50 mM NaCl and 0.05% Tween-20), and probed for 2 h with anti-plectin C-20 (Santa Cruz) diluted 1:400, anti-GAPDH (ab9484, Abcam) or anti-Lamin A (ab8980, Abcam) diluted 1:1000 or anti-FUS/TLS (ab23439, Abcam) diluted 1:2000. Detection was performed with AP-conjugated mouse-anti-goat antibody combined with BCIP/NBT substrate (Sigma-Aldrich), or with HRP-conjugated goat-anti-rabbit,

goat-anti-mouse or bovine-anti-goat antibodies combined with Supersignal West Dura (Pierce). Luminescent signals were captured with LAS 4000 and quantified using Image Gauge (Fujifilm).

In-gel protein digestion and nanoflow LC-MS/MS FT/ICR

Sample preparation and mass spectrometry analysis was performed at The Proteomics Core Facility at the Sahlgrenska Academy, University of Gothenburg. Briefly, gel pieces were destained by washing three times in 25 mM NH_4HCO_3 in 50% CH_3CN and once in 25 mM NH_4HCO_3 in 50% CH_3OH. Gel pieces were dried in a vacuum centrifuge and incubated with digestion buffer (50 mM NH_4HCO_3 and10 ng/μL trypsin) at 37 °C overnight. Peptides were extracted with 50% CH_3CN in 1% CH_3-COOH and dried completely. The peptides were reconstituted in 0.2% HCOOH, trapped on a pre-column (45 x × 0.075 mm i.d.) and separated on a reversed phase column; 200 × 0.050 mm packed with 3 μm Reprosil-Pur C_{18}-AQ particles. A 40 min gradient with 10–50% CH_3CN in 0.2% COOH was used for separation of the peptides. For more details see Carlsohn et. al. [26]. The nanoflow LC-MS/MS was performed on a hybrid linear ion trap-FTICR mass spectrometer equipped with a 7 T ICR magnet (LTQ-FT, Thermo Scientific). MS-spectra were acquired in the FTICR, while MS/MS-spectra were acquired in the LTQ-trap. For each scan of FTICR, the three most intense, doubly or triply charged, ions were sequentially fragmented in the linear trap by collision-induced dissociation. Tandem mass spectra were searched by MASCOT (Matrix Science) against the Swiss-prot database including all species. The search parameters were: MS accuracy 5 ppm, MS/MS accuracy 0.5 Da, one missed cleavage by trypsin allowed, fixed propionamide modification of cysteine and variable modification of oxidized methionine. Tryptic peptides matched at or above the 95% level of confidence were used to interpret data.

Immunofluorescence and proximity ligation assay

Cells were washed with PBS, fixed in methanol for 5 min, washed three times with PBS and incubated in blocking buffer (PBS pH 7.3, 5% BSA and 0.2% Triton X-100) for 30 min. For immunofluorescence cells were incubated 1 h at room temperature with anti-plectin (10 F6) diluted 1:50, anti-plectin (C-20) diluted 1:100, anti-TIA-1 (C-20), diluted 1:50 (all Santa Cruz) or anti-FUS/TLS (ab23439, Abcam) diluted 1:500 in blocking buffer. Cells were washed with PBS and incubated with goat-anti-mouse-CY3, goat-anti-rabbit-CY3 (Amersham) or donkey-anti-goat-AlexaFluor$_{568}$ (Invitrogen) all diluted 1:1000 in blocking buffer. Samples were washed in PBS and mounted using ProLong Gold with DAPI (Invitrogen). *In situ* proximity ligation assay (PLA) experiments were made using DuoLink II (Olink Bioscience). Cells were incubated overnight at 4 °C with anti-FUS/TLS (ab23439, Abcam) diluted 1:500 and/or anti-plectin (10 F6) diluted 1:50 in blocking buffer. Samples were then washed with PBS and incubated with PLA probes DII anti-mouse MINUS, DII anti-mouse PLUS, DII anti-rabbit MINUS or DII anti-rabbit PLUS in combinations suitable for single or dual recognition. Control experiments were included by omitting the primary antibody used for single recognition PLA or either one of the primary antibodies used in double recognition PLA. The subsequent washing steps, ligation, rolling-circle amplification and fluorescent labeling with DuoLink II Detection Reagent Orange were performed according to the manufacturers' instructions (Olink Bioscience). Slides with PLA samples were mounted in DuoLink II Mounting Media with DAPI (Olink Bioscience). A Zeiss LSM 510 META microscope equipped with a Zeiss image processing system was used for confocal imaging. A 63 ×/1.4 oil objective and sequential scanning with filters appropriate to each fluorophore was used (420–480 nm for DAPI, 505–530 nm for eGFP, 560–615 nm for CY3 and a long pass 560 nm for PLA signals). Images used for PLA quantification were captured and processed with identical settings. PLA signals of individual cells were counted with the Blob finder tool v3.2 [27] using 5 individual confocal images and a minimum of 50 cells per sample.

RNA extraction, cDNA synthesis and quantitative PCR

RNA was extracted and DNase treated using RNeasy Mini Kit (Qiagen). Total RNA concentration was measured using Nanodrop ND-1000 spectrophotometer (Nanodrop Technologies). Reverse transcription was performed with SuperScript III (Invitrogen). 6.5 μL samples containing ~100 ng total RNA, 0.5 mM dNTP (Sigma-Aldrich), 2.5 μM oligo(dT) and 2.5 μM random hexamers (Applied Biosystems) were incubated at 65 °C for 5 min. We then added 50 mM Tris–HCl (pH 8.3), 75 mM KCl, 3 mM $MgCl_2$, 5 mM dithiothreitol, 20 U RNaseOut and 100 U SuperScript III to a final volume of 10 μL (all Life Technologies/Invitrogen). The temperature profile used were 25 °C for 5 min, 50 °C for 1 h, 55 °C for 15 min and 70 °C for 15 min. Six negative controls without SuperScript III were included to test for genomic contamination. All samples were diluted with water to a final volume of 120 μL. Real-time PCR was performed with LightCycler 480 (Roche Diagnostics). Each 10 μL reaction contained 1 X iQ SYBR Green Supermix (Bio-Rad), 400 nM of each primer (Sigma-Aldrich) and 2 μL cDNA. Primer sequences were *Ash1l*: GAACACGGATGTGGAGCACTA (Fwd), ACAATCACCCTGACGAAGCAG (Rev); *Med12*: GACACCAAGGGCAACAAGAT (Fwd), ATGATAGAGCAACAGCCGC (Rev); *Shoc2*: GTTCTCTGCTTTCCTGCCTGTC (Fwd), TCAACTGGTAAAATGGTCCTGG (Rev). The temperature profile was 95 °C for 20 sec followed by 50 cycles of amplification (95 °C for 20 s, 60 °C for 20 s and 72 °C for 20 s). The formation of expected PCR products was confirmed by agarose gel electrophoresis and all samples were analyzed by melting curve analysis. Suitable reference genes were evaluated with NormFinder and the Reference Gene Panel Mouse (TATAA Biocenter). *Hprt*, *Gapdh* and *Tubb* were used as reference genes. The Reference Gene Panel was also used to show the effect of potential unregulated target genes (*Pgk1*, *Ppia* and *Ywhaz*). Data analysis was performed as previously described [28]. Statistical significance was determined using paired two tailed student *t*-test, differences were considered statistically significant when $P < 0.05$.

Results

The FUS N-terminal domain and plectin interact in vitro

To identify novel protein–protein interactions involving the FUS NTD, a bacterially expressed FUS-NTD GST fusion protein (Fig. 1a) was incubated with Raji protein extracts to capture interaction partners. SDS-PAGE analysis of sample eluates showed a high-molecular weight protein present in FUS-NTD-GST samples, but undetectable in controls (Fig. 1b). Mass spectrometry analysis

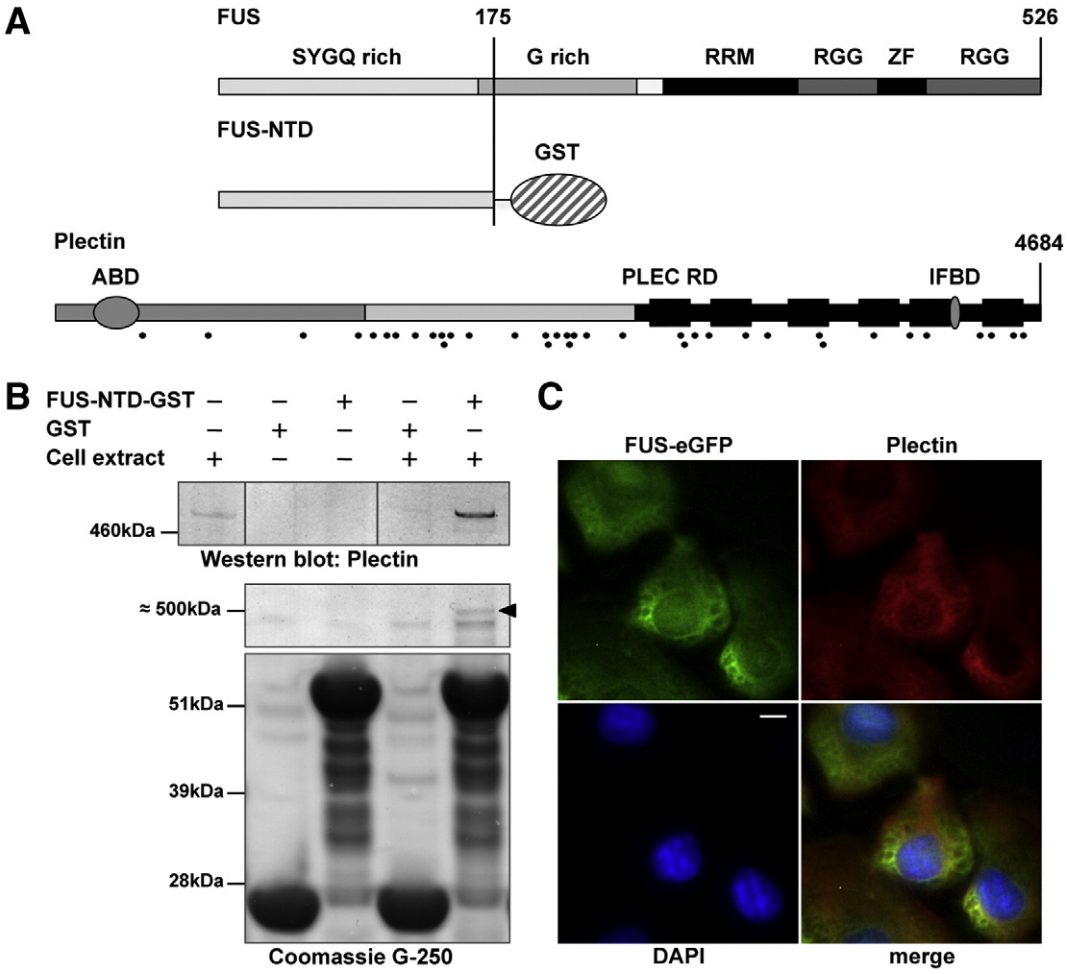

Fig. 1 – FUS and plectin interact *in vitro* and show overlapping cellular localization. A. Schematic representation of FUS (UniProt ID: P35637) domain structure and the recombinant FUS N-terminal domain (NTD) GST fusion protein. Plectin (UniProt ID: Q15149) is shown with domains defined by the SMART database. The globular N- and C-terminal domains and the central rod domain are shown by different shading. Dots indicate plectin derived peptides detected by mass spectrometry. Abbreviations for FUS are RRM: RNA recognition motif; RGG: RGG repeat domain; ZF: zinc finger domain. Abbreviations for plectin are PLEC RD: Plectin repeat domain; ABD: Actin binding domain and IFBD: Intermediate filament binding domain. Drawings are not to scale. B. Interaction of FUS and plectin demonstrated by pull-down. SDS-PAGE gel stained with Coomassie (lower panels) shows GST fusion proteins and a high molecular weight protein of approximately 500 kDa (arrowhead) specifically retained by the FUS-NTD bait and identified as plectin by mass spectrometry. Western blot (upper panel) analysis confirmed the enrichment of plectin in FUS-NTD-GST samples. C. Plectin (red) was visualized by immunofluorescence in fixed HT1080 cells with stable expression of FUS-eGFP (green). A partial overlap of FUS-eGFP and plectin was observed in the cytoplasm. Nuclei were stained with DAPI (blue). Scale bar is 10 μm.

of tryptic digests revealed that the majority of peptides were derived from human plectin (Fig. 1a). Western blot with a plectin specific antibody verified the protein identity and the specific interaction of plectin with the FUS NTD *in vitro* (Fig. 1b). Similar experiments were performed using recombinant proteins of the EWSR1 and TAF15 NTDs that also resulted in capture of plectin as determined by Western blot analysis (Supplementary Fig. 1).

FUS-eGFP and plectin localization overlap in the cytoplasm

HT1080 fibrosarcoma cells with stable expression of FUS-eGFP were stained by indirect immunofluorescence using antibodies for plectin (Fig. 1c). FUS-eGFP showed a nucleocytoplasmic distribution identical to endogenous FUS [18], while plectin was detected exclusively in the cytoplasmic domain as previously reported [29]. A partial overlap was observed for the staining pattern of plectin and the FUS-eGFP signal in the cytoplasm, suggesting that FUS-plectin interaction may occur. No difference in plectin distribution was observed when comparing unmodified HT1080 and cells expressing FUS-eGFP (data not shown).

FUS and plectin are in close proximity in situ

Fixed HT1080 cells were analyzed by proximity ligation assay (PLA) with a combination of FUS and plectin specific antibodies to further characterize the FUS-plectin interaction *in situ* (Fig. 2). The PLA

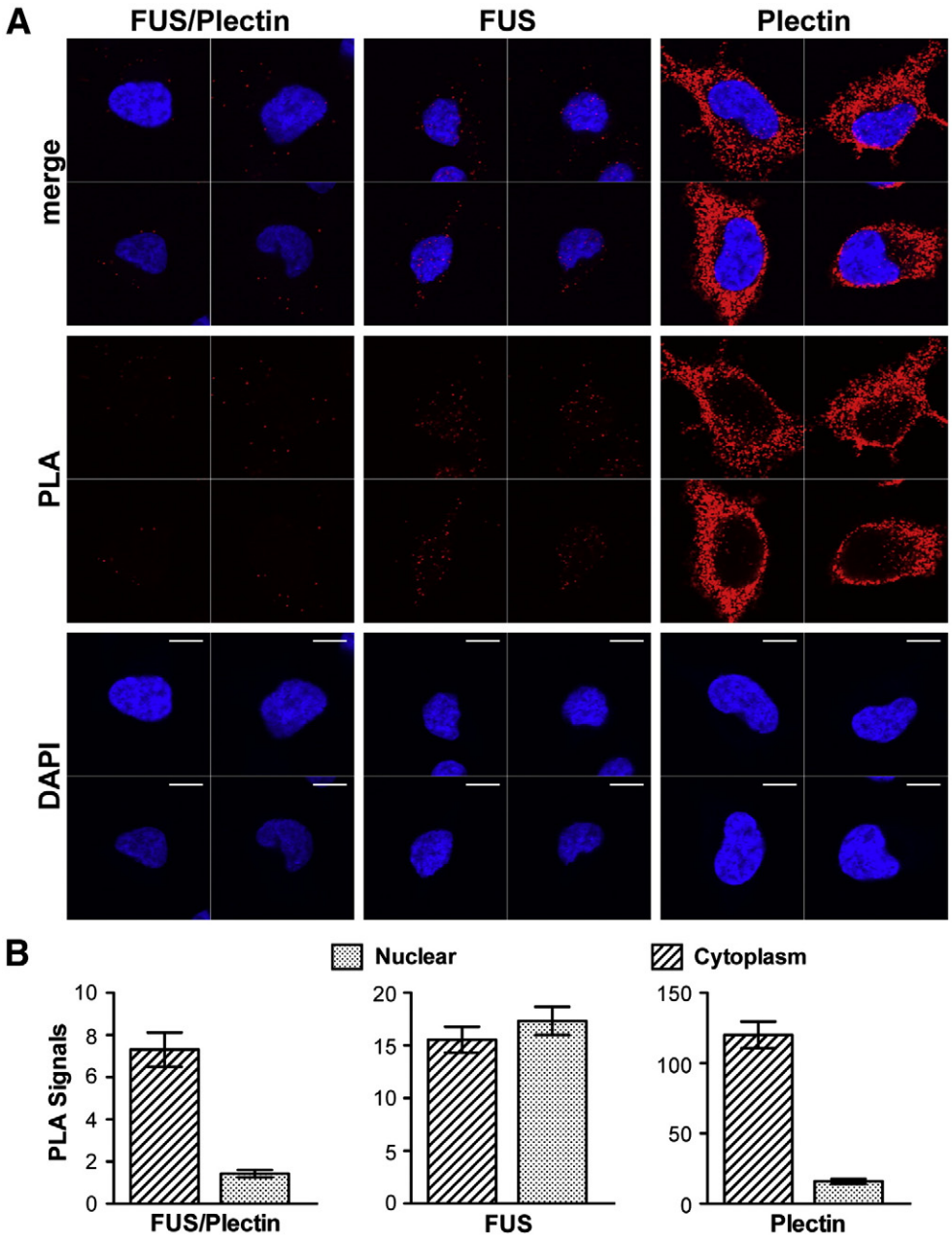

Fig. 2 – FUS and plectin are in close proximity *in situ*. A. Double recognition *in situ* PLA (left panels) detected FUS and plectin protein molecules in close proximity in the cytoplasm, indicating physical interaction. Single recognition *in situ* PLA shows a nucleo-cytoplasmic distribution of FUS (middle panels), while plectin (right panels) is pre-dominantly localized in the cytoplasm. Scale bars are 10 μm. B. The number of PLA signals per cell of the cytoplasm and nuclei was quantified. Note that count values for PLA signals are arbitrary and not directly comparable for different samples neither in the PLA quantification (B) nor to the visualization (A). Number of cells analyzed was 50–75 per sample, mean +/− SEM is shown. Control experiments for PLA specificity are shown in Supplementary Fig. 2.

signals formed showed that FUS and plectin were closely associated in the cytoplasm. To verify the PLA results, FUS and plectin were analyzed with single primary antibodies (Fig. 2). We found that the subcellular localization of FUS and plectin PLA signals was in agreement with the previous immunostaining (Fig. 1c). Negative controls were included for all experiments to exclude the possibility of detecting unspecific PLA signals (Supplementary Fig. 2).

FUS localization and expression of FUS bound mRNAs are altered in cells lacking plectin

To address the functional importance of the FUS–plectin interaction we compared FUS expression levels and subcellular localization in wildtype and plectin knockout mouse fibroblasts using immunofluorescence analysis (Fig. 3a) and subcellular fractionation followed

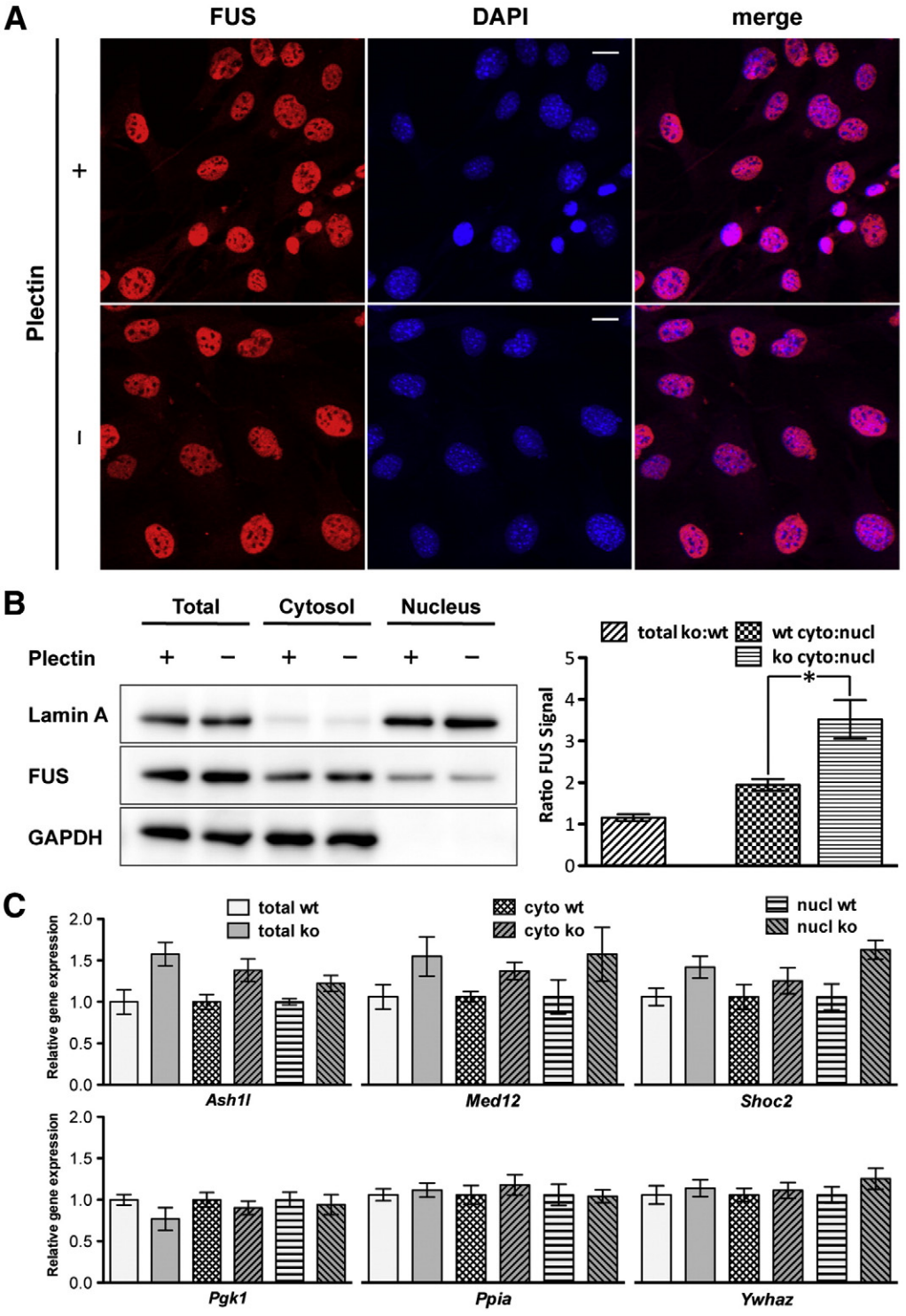

Fig. 3 – The subcellular distribution and function of FUS is altered in plectin knockout cells. A. Visualization of FUS expression in wildtype (+) and plectin knockout (−) mouse fibroblasts by immunofluorescence. Scale bars are 20 μm. B. Western blot analysis of FUS in cytosolic and nuclear fractions from wildtype (+) and plectin knockout (−) cells (left). Purity of fractions was determined by antibodies to Lamin A (nuclear) and GADPH (cytosolic). The quantity of FUS was determined by chemiluminescence of bound antibodies (right), bars are mean values ± SEM of 4 experiments. The ratio of FUS derived signal for wildtype (wt) to plectin knockout (ko) total protein samples indicates no significant difference in FUS expression. However, the ratio of cytosolic to nuclear FUS signal is higher in cells lacking plectin indicating an altered distribution of FUS. Statistical significance was determined by Mann–Whitney (*$p < 0.05$). C. The expression level of mRNAs known to associate with FUS (*Ash1l*, *Med12*, *Shoc2*) was increased in plectin knockout cells compared to wildtype cells as determined by real time quantitative PCR analysis of RNA preparations from samples in B. Control transcripts (*Pgk1*, *Ppia*, *Ywhaz*) did not show any altered expression in cells lacking plectin. All wildtype expression values were arbitrarily set to 1.

by Western blot (Fig. 3b). Western blot analysis revealed that the cytoplasmic to nuclear ratio of FUS protein level was increased in cells lacking plectin, while the total level of FUS was unaffected. The immunofluorescence analysis revealed no clear visual difference between wildtype and knockout cells. The indication that FUS localization was altered in the absence of plectin prompted us to investigate FUS mediated gene regulation. We analyzed the expression levels of *Ash1l*, *Med12* and *Shock2* transcripts, which have been reported to interact with FUS [19], and found all to be up regulated in plectin knockout cells, while assumed non-target mRNAs (*Pgk1*, *Ppia* and *Ywhaz*,) of FUS were unaffected (Fig. 3c). These results indicate that plectin is required for normal localization and function of FUS.

Discussion

In this study we have identified a novel interaction between the RNA binding protein FUS and the cytolinker plectin. Furthermore, we demonstrate that plectin expression is required for correct subcellular localization and function of FUS.

Plectin is a large protein (>500 kDa), belonging to the Plakin family that control cytoskeleton organization and mechanical stability of cells [29–31]. The functional importance of plectin is most obviously revealed in patients carrying plectin mutations leading to epidermolysis bullosa (EB) with blistering and fragility of the skin, and in the case of plectin associated EB also involves the neuromuscular system [32]. Plectin is composed of a long central coiled-coil rod structure flanked by globular N- and C-terminal domains [33] (Fig. 1a). The N-terminal domain interacts with actin and microtubule [34], while the C-terminal associates with intermediate filaments [33]. The interaction with the cytoskeleton and its function as a cross-linker explains plectin's importance to cellular stability and organization [29,31,35]. However, plectin also acts as a scaffold for proteins involved in signaling [36–38]. In our study plectin was isolated by affinity capture using the FUS NTD that shares a high degree of sequence homology with the other FET family members EWSR1 and TAF15. We also demonstrated that the interaction with plectin is conserved for all FET proteins *in vitro*, but the significance of EWSR1 and TAF15 binding to plectin was not further investigated. Immunofluorescence analysis of HT1080 cells expressing eGFP-tagged FUS showed a partial overlap of FUS-eGFP and plectin in the cytoplasm. The interaction of endogenous FUS and plectin was further investigated by *in situ* PLA concluding that the proteins are close enough to interact directly or associate with common complexes in the cytoplasm. The subcellular localization of plectin was unaffected when FUS(−eGFP) was over expressed, indicating that plectin dictates the localization were interaction occurs (data not shown). Previous reports provide indirect support for our observations. Plectin is located at adhesion complexes [29,39,40], an observation that is shared with FUS and other FET proteins [18,41] that localizes to spreading initiation centers during early stages of cell adhesion. Furthermore, plectin is an interaction partner of RACK1 [37] that also co-localizes with FUS, EWSR1 and TAF15 in spreading initiation centers [18]. Perturbation of RNA binding proteins in general (and FUS in particular) affects cell spreading indicating that FUS, as plectin, is involved in cell adhesion [41]. The neural isoform of plectin (plectin 1 C) is localized to adhesion complexes in postsynaptic dendrites mediating connections with axons [42], while FUS also localizes to dendrites as a member of complexes carrying mRNA by microtubule mediated transport [19,20,43]. The mRNA transport maintains localized translation and protein synthesis in dendrites and is augmented by synaptic excitation [20]. Taken together, our results and that FUS and plectin localize to common sites, suggest that plectin acts as a scaffold for FUS and facilitates its delivery of mRNA to specific locations. Localized translation is an established concept in neurons [44], but also likely to be an important mechanism for other cell types [45]. In agreement with this notion, we show that mouse fibroblasts lacking plectin display a change in FUS cellular localization and altered expression levels of mRNAs previously described to interact with FUS [19] (Fig. 3). Transcripts that, to our knowledge, do not interact with FUS or the other FET proteins did not show any change in expression levels. The accumulation of transcripts in plectin deficient cells may be a consequence of mRNA molecules failing to reach their specific target destination, when FUS mediated transport is compromised. This could lead to transcriptional upregulation of mRNAs by feedback mechanisms. Alternatively, the change in FUS subcellular distribution may be associated with a reduction of FUS regulated transcriptional activity in the nucleus that directly affects the abundance of selected transcripts. Several plectin isoforms exist that exhibit differences in subcellular localization [46] and could recruit FUS to various sites depending on the requirements of different cell types. It is possible that localized translation is affected when plectin function is compromised and that impaired synthesis or protein targeting to the cell membrane may contribute to symptoms that are specific for the type of EB caused by plectin deficiency. It is interesting to note that FUS and the other FET family proteins have been reported to associate with a substantial repertoire of transcripts [17], therefore, our observed deregulation of gene expression in plectin deficient cells probably extend beyond the transcripts evaluated in our study.

Mutations in *FUS* are causative of ALS and FTLD [5–7] and linked to changes in FUS nucleocytoplasmic shuttling and FUS immunoreactive inclusions in the cytoplasm [5,6,47,48]. C-terminal mutations in FUS are reported to affect a nuclear localization signal and cause cytoplasmic accumulation of FUS and formation of abnormal stress granules resembling ALS/FTLD inclusion bodies [49]. The dramatic accumulation of mutated FUS in ALS tissues may disturb plectin and its interaction with other proteins, thus spreading the mutation effects to the cytoskeletal system. The interaction of plectin with the cytoskeleton and that stress granule assembly is dependent on functional microtubules [50,51] prompted us to investigate plectin's role in stress granule formation. HT1080 cells showed formation of stress granules (defined by FUS-eGFP and TIA-1 staining [18]) following arsenite treatment, while staining for plectin did not reveal any change in protein levels or localization (data not shown). However, the result does not exclude a role for plectin in FUS localization and transport in other cell types or under other conditions. Furthermore, plectin interacts indirectly with nuclear pore complexes (NPCs) through Nesprin-3α [52] and SUN proteins residing in the nuclear membrane [53,54]. We isolated plectin by its affinity for the FUS N-terminal, thus adjacent mutations in the FUS N-terminal domain may affect interaction with plectin and FUS transport via NPCs. The mislocalization of FUS and deregulation of mRNAs interacting with FUS [19] in cells lacking plectin may be explained by an obstruction of FUS transport over the nuclear membrane.

In summary, we have identified an interaction of the RNA binding protein FUS and the cytolinker plectin occurring in the cytoplasm. Lack of plectin caused changes in FUS subcellular localization and the expression of FUS bound mRNAs. We hypothesize that plectin functions as a scaffold to facilitate transport and targeting of FUS and its associated mRNAs. The significance of the FUS–plectin interaction in relation to ALS, FTLD and EB pathology warrant further investigation.

Acknowledgments

We acknowledge the Proteomics Core Facility and the Centre for Cellular Imaging both at the Sahlgrenska Academy, University of Gothenburg for their services, use of equipment and technical support. This work was financially supported by the Swedish Cancer Society, the Swedish Research Council (AS, K2012-99X-21954-01-3), the Swedish Society for Medical Research, Socialstyrelsen, the BioCARE National Strategic Research Program at University of Gothenburg, the Assar Gabrielssons Research Foundation, the Johan Jansson Foundation for Cancer Research, the Wilhelm and Martina Lundgrens Foundation and the Sigurd and Elsa Goljes Foundation.

Appendix A. Supplementary data

Supplementary data to this article can be found online at doi:10.1016/j.yexcr.2011.12.019.

REFERENCES

[1] A. Crozat, P. Aman, N. Mandahl, D. Ron, Fusion of CHOP to a novel RNA-binding protein in human myxoid liposarcoma, Nature 363 (1993) 640–644.
[2] P. Aman, D. Ron, N. Mandahl, T. Fioretos, S. Heim, K. Arheden, H. Willen, A. Rydholm, F. Mitelman, Rearrangement of the transcription factor gene CHOP in myxoid liposarcomas with t(12;16)(q13;p11), Genes Chromosomes Cancer 5 (1992) 278–285.
[3] T.H. Rabbitts, A. Forster, R. Larson, P. Nathan, Fusion of the dominant negative transcription regulator CHOP with a novel gene FUS by translocation t(12;16) in malignant liposarcoma, Nat. Genet. 4 (1993) 175–180.
[4] N. Riggi, L. Cironi, M.L. Suva, I. Stamenkovic, Sarcomas: genetics, signalling, and cellular origins. Part 1: the fellowship of TET, J. Pathol. 213 (2007) 4–20.
[5] C. Vance, B. Rogelj, T. Hortobagyi, K.J. De Vos, A.L. Nishimura, J. Sreedharan, X. Hu, B. Smith, D. Ruddy, P. Wright, J. Ganesalingam, K.L. Williams, V. Tripathi, S. Al-Saraj, A. Al-Chalabi, P.N. Leigh, I.P. Blair, G. Nicholson, J. de Belleroche, J.M. Gallo, C.C. Miller, C.E. Shaw, Mutations in FUS, an RNA processing protein, cause familial amyotrophic lateral sclerosis type 6, Science 323 (2009) 1208–1211.
[6] T.J. Kwiatkowski Jr., D.A. Bosco, A.L. Leclerc, E. Tamrazian, C.R. Vanderburg, C. Russ, A. Davis, J. Gilchrist, E.J. Kasarskis, T. Munsat, P. Valdmanis, G.A. Rouleau, B.A. Hosler, P. Cortelli, P.J. de Jong, Y. Yoshinaga, J.L. Haines, M.A. Pericak-Vance, J. Yan, N. Ticozzi, T. Siddique, D. McKenna-Yasek, P.C. Sapp, H.R. Horvitz, J.E. Landers, R.H. Brown Jr., Mutations in the FUS/TLS gene on chromosome 16 cause familial amyotrophic lateral sclerosis, Science 323 (2009) 1205–1208.
[7] C. Lagier-Tourenne, M. Polymenidou, D.W. Cleveland, TDP-43 and FUS/TLS: emerging roles in RNA processing and neurodegeneration, Hum. Mol. Genet. 19 (2010) R46–R64.
[8] S. Yang, S.T. Warraich, G.A. Nicholson, I.P. Blair, Fused in sarcoma/translocated in liposarcoma: a multifunctional DNA/RNA binding protein, Int. J. Biochem. Cell Biol. 42 (2010) 1408–1411.
[9] P. Aman, I. Panagopoulos, C. Lassen, T. Fioretos, M. Mencinger, H. Toresson, M. Hoglund, A. Forster, T.H. Rabbitts, D. Ron, N. Mandahl, F. Mitelman, Expression patterns of the human sarcoma-associated genes FUS and EWS and the genomic structure of FUS, Genomics 37 (1996) 1–8.
[10] D. Perrotti, S. Bonatti, R. Trotta, R. Martinez, T. Skorski, P. Salomoni, E. Grassilli, R.V. Lozzo, D.R. Cooper, B. Calabretta, TLS/FUS, a pro-oncogene involved in multiple chromosomal translocations, is a novel regulator of BCR/ABL-mediated leukemogenesis, EMBO J. 17 (1998) 4442–4455.
[11] A.Y. Tan, J.L. Manley, The TET family of proteins: functions and roles in disease, J. Mol. Cell Biol. 1 (2009) 82–92.
[12] N. Ticozzi, C. Vance, A.L. Leclerc, P. Keagle, J.D. Glass, D. McKenna-Yasek, P.C. Sapp, V. Silani, D.A. Bosco, C.E. Shaw, R.H. Brown Jr., J.E. Landers, Mutational analysis reveals the FUS homolog TAF15 as a candidate gene for familial amyotrophic lateral sclerosis, Am. J. Med. Genet. B Neuropsychiatr. Genet. 156B (2011) 285–290.
[13] H. Uranishi, T. Tetsuka, M. Yamashita, K. Asamitsu, M. Shimizu, M. Itoh, T. Okamoto, Involvement of the pro-oncoprotein TLS (translocated in liposarcoma) in nuclear factor-kappa B p65-mediated transcription as a coactivator, J. Biol. Chem. 276 (2001) 13395–13401.
[14] X. Wang, S. Arai, X. Song, D. Reichart, K. Du, G. Pascual, P. Tempst, M.G. Rosenfeld, C.K. Glass, R. Kurokawa, Induced ncRNAs allosterically modify RNA-binding proteins in cis to inhibit transcription, Nature 454 (2008) 126–130.
[15] L. Yang, L.J. Embree, S. Tsai, D.D. Hickstein, Oncoprotein TLS interacts with serine-arginine proteins involved in RNA splicing, J. Biol. Chem. 273 (1998) 27761–27764.
[16] H. Zinszner, J. Sok, D. Immanuel, Y. Yin, D. Ron, TLS (FUS) binds RNA in vivo and engages in nucleocytoplasmic shuttling, J. Cell Sci. 110 (Pt 15) (1997) 1741–1750.
[17] J.I. Hoell, E. Larsson, S. Runge, J.D. Nusbaum, S. Duggimpudi, T.A. Farazi, M. Hafner, A. Borkhardt, C. Sander, T. Tuschl, RNA targets of wild-type and mutant FET family proteins, Nat. Struct. Mol. Biol. 18 (2011) 1428–1431.
[18] M.K. Andersson, A. Stahlberg, Y. Arvidsson, A. Olofsson, H. Semb, G. Stenman, O. Nilsson, P. Aman, The multifunctional FUS, EWS and TAF15 proto-oncoproteins show cell type-specific expression patterns and involvement in cell spreading and stress response, BMC Cell Biol. 9 (2008) 37.
[19] R. Fujii, T. Takumi, TLS facilitates transport of mRNA encoding an actin-stabilizing protein to dendritic spines, J. Cell Sci. 118 (2005) 5755–5765.
[20] R. Fujii, S. Okabe, T. Urushido, K. Inoue, A. Yoshimura, T. Tachibana, T. Nishikawa, G.G. Hicks, T. Takumi, The RNA binding protein TLS is translocated to dendritic spines by mGluR5 activation and regulates spine morphology, Curr. Biol. 15 (2005) 587–593.
[21] P. Anderson, N. Kedersha, RNA granules: post-transcriptional and epigenetic modulators of gene expression, Nat. Rev. Mol. Cell Biol. 10 (2009) 430–436.
[22] J. Woulfe, D.A. Gray, I.R. Mackenzie, FUS-immunoreactive intranuclear inclusions in neurodegenerative disease, Brain Pathol. 20 (2010) 589–597.
[23] D.G. Munoz, M. Neumann, H. Kusaka, O. Yokota, K. Ishihara, S. Terada, S. Kuroda, I.R. Mackenzie, FUS pathology in basophilic inclusion body disease, Acta Neuropathol. 118 (2009) 617–627.
[24] K.A. Lee, Ewing's family oncoproteins: drunk, disorderly and in search of partners, Cell Res. 17 (2007) 286–288.

[25] H.J. Dyson, P.E. Wright, Intrinsically unstructured proteins and their functions, Nat. Rev. Mol. Cell Biol. 6 (2005) 197–208.
[26] E. Carlsohn, J. Nystrom, H. Karlsson, A.M. Svennerholm, C.L. Nilsson, Characterization of the outer membrane protein profile from disease-related *Helicobacter pylori* isolates by subcellular fractionation and nano-LC FT-ICR MS analysis, J. Proteome Res. 5 (2006) 3197–3204.
[27] A. Allalou, C. Wahlby, BlobFinder, a tool for fluorescence microscopy image cytometry, Comput. Methods Programs Biomed. 94 (2009) 58–65.
[28] A. Stahlberg, K. Elbing, J.M. Andrade-Garda, B. Sjogreen, A. Forootan, M. Kubista, Multiway real-time PCR gene expression profiling in yeast *Saccharomyces cerevisiae* reveals altered transcriptional response of ADH-genes to glucose stimuli, BMC Genomics 9 (2008) 170.
[29] G. Wiche, Role of plectin in cytoskeleton organization and dynamics, J. Cell Sci. 111 (Pt 17) (1998) 2477–2486.
[30] A. Sonnenberg, R.K. Liem, Plakins in development and disease, Exp. Cell Res. 313 (2007) 2189–2203.
[31] S. Na, F. Chowdhury, B. Tay, M. Ouyang, M. Gregor, Y. Wang, G. Wiche, N. Wang, Plectin contributes to mechanical properties of living cells, Am. J. Physiol. Cell Physiol. 296 (2009) C868–C877.
[32] E. Pfendner, F. Rouan, J. Uitto, Progress in epidermolysis bullosa: the phenotypic spectrum of plectin mutations, Exp. Dermatol. 14 (2005) 241–249.
[33] L. Janda, J. Damborsky, G.A. Rezniczek, G. Wiche, Plectin repeats and modules: strategic cysteines and their presumed impact on cytolinker functions, Bioessays 23 (2001) 1064–1069.
[34] F.A. Steinbock, G. Wiche, Plectin: a cytolinker by design, Biol. Chem. 380 (1999) 151–158.
[35] K. Andra, B. Nikolic, M. Stocher, D. Drenckhahn, G. Wiche, Not just scaffolding: plectin regulates actin dynamics in cultured cells, Genes Dev. 12 (1998) 3442–3451.
[36] S. Osmanagic-Myers, M. Gregor, G. Walko, G. Burgstaller, S. Reipert, G. Wiche, Plectin-controlled keratin cytoarchitecture affects MAP kinases involved in cellular stress response and migration, J. Cell Biol. 174 (2006) 557–568.
[37] S. Osmanagic-Myers, G. Wiche, Plectin-RACK1 (receptor for activated C kinase 1) scaffolding: a novel mechanism to regulate protein kinase C activity, J. Biol. Chem. 279 (2004) 18701–18710.
[38] M. Gregor, A. Zeold, S. Oehler, K.A. Marobela, P. Fuchs, G. Weigel, D.G. Hardie, G. Wiche, Plectin scaffolds recruit energy-controlling AMP-activated protein kinase (AMPK) in differentiated myofibres, J. Cell Sci. 119 (2006) 1864–1875.
[39] K. Andra, I. Kornacker, A. Jorgl, M. Zorer, D. Spazierer, P. Fuchs, I. Fischer, G. Wiche, Plectin-isoform-specific rescue of hemidesmosomal defects in plectin (−/−) keratinocytes, J. Invest Dermatol. 120 (2003) 189–197.
[40] G.J. Seifert, D. Lawson, G. Wiche, Immunolocalization of the intermediate filament-associated protein plectin at focal contacts and actin stress fibers, Eur. J. Cell Biol. 59 (1992) 138–147.
[41] C.L. de Hoog, L.J. Foster, M. Mann, RNA and RNA binding proteins participate in early stages of cell spreading through spreading initiation centers, Cell 117 (2004) 649–662.
[42] P. Fuchs, M. Zorer, S. Reipert, G.A. Rezniczek, F. Propst, G. Walko, I. Fischer, J. Bauer, M.W. Leschnik, B. Luscher, J.G. Thalhammer, H. Lassmann, G. Wiche, Targeted inactivation of a developmentally regulated neural plectin isoform (plectin 1c) in mice leads to reduced motor nerve conduction velocity, J. Biol. Chem. 284 (2009) 26502–26509.
[43] Y. Kanai, N. Dohmae, N. Hirokawa, Kinesin transports RNA: isolation and characterization of an RNA-transporting granule, Neuron 43 (2004) 513–525.
[44] I.G. Macara, H. Iioka, S. Mili, Axon growth-stimulus package includes local translation, Nat. Cell Biol. 11 (2009) 919–921.
[45] D.E. Willis, J.L. Twiss, Regulation of protein levels in subcellular domains through mRNA transport and localized translation, Mol. Cell Proteomics 9 (2010) 952–962.
[46] G.A. Rezniczek, C. Abrahamsberg, P. Fuchs, D. Spazierer, G. Wiche, Plectin 5′-transcript diversity: short alternative sequences determine stability of gene products, initiation of translation and subcellular localization of isoforms, Hum. Mol. Genet. 12 (2003) 3181–3194.
[47] D.A. Bosco, N. Lemay, H.K. Ko, H. Zhou, C. Burke, T.J. Kwiatkowski Jr., P. Sapp, D. McKenna-Yasek, R.H. Brown Jr., L.J. Hayward, Mutant FUS proteins that cause amyotrophic lateral sclerosis incorporate into stress granules, Hum. Mol. Genet. 19 (2010) 4160–4175.
[48] J. Gal, J. Zhang, D.M. Kwinter, J. Zhai, H. Jia, J. Jia, H. Zhu, Nuclear localization sequence of FUS and induction of stress granules by ALS mutants, Neurobiol. Aging 32 (2010) 27–40.
[49] D. Dormann, R. Rodde, D. Edbauer, E. Bentmann, I. Fischer, A. Hruscha, M.E. Than, I.R. Mackenzie, A. Capell, B. Schmid, M. Neumann, C. Haass, ALS-associated fused in sarcoma (FUS) mutations disrupt transportin-mediated nuclear import, EMBO J. 29 (2010) 2841–2857.
[50] P.A. Ivanov, E.M. Chudinova, E.S. Nadezhdina, Disruption of microtubules inhibits cytoplasmic ribonucleoprotein stress granule formation, Exp. Cell Res. 290 (2003) 227–233.
[51] E.S. Nadezhdina, A.J. Lomakin, A.A. Shpilman, E.M. Chudinova, P.A. Ivanov, Microtubules govern stress granule mobility and dynamics, Biochim. Biophys. Acta 1803 (2010) 361–371.
[52] K. Wilhelmsen, S.H. Litjens, I. Kuikman, N. Tshimbalanga, H. Janssen, I. van den Bout, K. Raymond, A. Sonnenberg, Nesprin-3, a novel outer nuclear membrane protein, associates with the cytoskeletal linker protein plectin, J. Cell Biol. 171 (2005) 799–810.
[53] M. Ketema, K. Wilhelmsen, I. Kuikman, H. Janssen, D. Hodzic, A. Sonnenberg, Requirements for the localization of nesprin-3 at the nuclear envelope and its interaction with plectin, J. Cell Sci. 120 (2007) 3384–3394.
[54] Q. Liu, N. Pante, T. Misteli, M. Elsagga, M. Crisp, D. Hodzic, B. Burke, K.J. Roux, Functional association of Sun1 with nuclear pore complexes, J. Cell Biol. 178 (2007) 785–798.